RESOURCECODE

MARINE DATA TOOLBOX

RESOURCECODE

Resource Characterization to Reduce the Cost of Energy through Coordinated Data Enterprise

WAVE HINDCAST DATABASE USER MANUAL

Issue : 1.3

Contributors : Accensi Mickaël, Alday Matias, Maisondieu Christophe
Approval date : March 2022

EMEC THE EUROPEAN MARINE ENERGY CENTRE LTD

CENTRALE NANTES

ODL

BLUEWISE MARINE

INNOSEA An LDC Group company

Ifremer

THE UNIVERSITY of EDINBURGH

UCD DUBLIN

Revision

Revision no.	Revision Text	Initials	Date
1.0	Creation	M. Alday	25/02/2020
1.1	Update	M. Accensi	20/07/2021
1.2	Submission	M. Accensi	31/08/2021
1.3	Review	C. Maisondieu	09/09/2021

Project Information

Project title	Resource Characterization to Reduce the Cost of Energy through Coordinated Data Enterprise
Project Acronym	RESOURCECODE
Project Number	ESES-5030
Duration	36 months
Month 1	Dec 2018
Project manager	Ruari Brooker | EMEC
Work package leader	Mickael Accensi | IFREMER
Work package number/name	WP3| Database development
Date of submission	31/08/2021

RESOURCECODE Consortium

Organization name	Country
European Marine Energy Centre (EMEC)	UK
IFREMER	France
OceanDataLab	France
Blue Wise Marine	Ireland
Centrale Nantes	France
University College Dublin	Ireland
See-d	France
University of Edinburgh	UK
INNOSEA	France

Contents

List of Figures

List of Tables

Abbreviations

Abbreviation	Definition
MARINE RENEWABLE ENERGY	MRE
RESEARCH TECHNOLOGY DEVELOPMENT	RTD
TECHNOLOGY READINESS LEVELS	TRL
OCEAN RENEWABLE ENERGY	ORE
WAVEWATCH-III ®	WW3

1 Introduction

The RESOURCECODE wave database was developed at Ifremer by the Laboratory of Ocean Physics and Satellite remote sensing (LOPS by its acronym in French). The generated hindcast was also primarily validated at Ifremer by LOPS and the Marine Structures Laboratory (LCSM by its acronym in French), and further analyzed at the Laboratory of Hydrodynamics, Energy and Atmospheric Environment at Ecole Centrale Nantes.

This high-resolution regional hindcast includes the evolution in time (hourly) and space of the directional spectrum and several integrated wave parameters, which allow to have a detailed description of the sea states. The modelled area extends from 12°W to 13.5°E longitude, and from 36°N to 63°N latitude, hence, the European and UK's North Atlantic coast, Irish sea, the Northern Sea, and La Manche are included within the domain. On its first version (March 2021), this data-set covers 27 years from 1994 to 2020.

The primary aim of the RESOURCECODE project is the creation of a marine data toolbox to enable developers of ocean energy devices and arrays, and their suppliers, to make optimized technical and commercial decisions, but the open nature of the wave database created allows its use in diverse research and/or engineering applications.

It must be highlighted that the RESOURCECODE database can be considered as an extension (geographically and in time) of its predecessor, the HOMERE database, which final update was completed in 2017 (https://doi.org/10.12770/cf47e08d-1455-4254-955e-d66225c9dc90).

2 Model Description

The wave database was generated utilizing the spectral model WAVEWATCH III ® (WW3DG, 2019) version 7.08. WAVEWATCH III (from hereon WW3) integrates, in space and time, the Eulerian representation of the wave action equation on its conservative form. Wave propagation is represented by the local rate of change, while spatial and spectral transport terms are balanced by the non-conservative sources and sinks (in general called source terms). The balance equation of the wave action $N(\kappa,\theta;\boldsymbol{x},t)$ in WW3 is given as:

$$\partial N\partial t+\nabla x\cdot x.N+\partial\partial\kappa\kappa.N+\partial\partial\theta\theta.N=S\sigma\partial N\partial t+\nabla x\cdot x.N+\partial\partial\kappa\kappa.N+\partial\partial\theta\theta.N=S\sigma \quad (1)$$

$$N=N(\kappa,\theta;x,t)N=N(\kappa,\theta;x,t) \quad (2)$$

$$x.=cg+Ux.=cg+U \tag{3}$$

$$\kappa.=-\partial\sigma\partial d\partial d\partial s-\kappa\cdot(\partial U\partial s)\kappa.=-\partial\sigma\partial d\partial d\partial s-\kappa\cdot(\partial U\partial s) \tag{4}$$

$$\theta.=1\kappa[\partial\sigma\partial d\partial d\partial m]+k\cdot(\partial U\partial m)\theta.=1\kappa[\partial\sigma\partial d\partial d\partial m]+k\cdot(\partial U\partial m) \tag{5}$$

where:

C_g: group celerity [m/s]

S: source terms

σ: wave angular frequency [rad/s]

k: wave number vector [rad/m]

U: current vector [m/s]

θ: wave direction [°]

s: coordinate in the direction of θ

m: coordinate perpendicular to **s**

Equation (1) is valid for Cartesian coordinates. For large scale applications, this equation is usually expressed in spherical coordinates.

In deep water conditions, the net source term **S** consists generally of three parts, an atmosphere-wave interaction term $\mathbf{S_{in}}$, which is usually a positive energy input, a non-linear wave-wave interactions term $\mathbf{S_{nl}}$ and a wave-ocean interaction term that generally contains dissipation $\mathbf{S_{ds}}$. In shallow water additional processes are considered, the most commons are wave-bottom interactions $\mathbf{S_{bot}}$, depth induced breaking $\mathbf{S_{db}}$ in extremely shallow water and triad wave-wave interactions $\mathbf{S_{tr}}$. The net source term **S** can be expressed as:

$$S=Sin+Snl+Sds+Sbot+Sdb+Str+... \tag{6}$$

The source terms considered in equation (6), and their different expressions will depend on the physical parameterizations selected in the WW3 compilation. For

further details on the WW3 equations and parameterizations, please refer to the User manual and system documentation of WAVEWATCH III® version 6.07.

2.1 Parameterizations

The physical parameters used for generation and dissipation of wave energy correspond to the ones specified in WW3 source terms package ST4, described in Ardhuin et al. (2010) and updated by Leckler et al. (2013). This parameterization has the following main features:

Discrete interaction approximation (Hasselmann et al., 1985) for non-linear wave-wave interactions.

Separated dissipation of swell (negative wind input) and dissipation due to wave breaking following Tolman & Chalikov (1996).

Breaking-induced dissipation based on the local saturation spectrum following Phillips (1984).

Sheltering term used to reduce the effective wind input for shorter waves (Chen and Belcher, 2000; Banner and Morison, 2010).

Cumulative dissipation rate directly estimated from breaking wave probabilities (concept taken from Babanin and Young; 2005).

Improved non-linear swell dissipation based on satellite observations (SAR derived dissipation rates) described in Ardhuin et al. (2009).

In addition, the WW3 BT4 option for wave dissipation due to bottom friction (S_{bot}) is used. This includes a more realistic estimation for sandy bottoms based on the eddy viscosity model by Grant and Madsen (1979) and a roughness parametrization that includes the formation of ripples and transition to sheet flow. The parametrization of Tolman (1994) was adjusted by Ardhuin et al. (2003) using field measurements from the DUCK’94 and SHOWEX experiments. In WW3, this approach has been adapted by including a sub-grid parametrization to take into account the variability of the water depth (Tolman;1995b).

2.2 Discretization and setup

The wave spectrum discretization considers 36 frequencies, starting from 0.0339 [Hz] up to 0.9526 [Hz] with a frequency increment factor of 1.1 and, in terms of directional discretization, 36 directions were used (equivalent to a directional resolution of 10°; see Figure 1).

Wave propagation is performed over an unstructured mesh with an explicit numerical scheme (Roland, 2008; Roland, 2009). Since a triangle-based mesh is

employed, the model's spatial resolution varies throughout the domain, subjected to depth changes and CFL defined restrictions to optimize node distribution, and ensure numerical stability. The minimum node distance in the mesh is ~300 [m] at coast lines and refined areas, while the largest triangle side can reach ~20 [km] in deep waters.

CFL conditions, as well as the minimum, maximum and refraction time steps, were defined following the WW3 recommendations, taking into account the minimum mesh spatial resolution and the fact that tidal currents are used to account for wave-current interaction effects (see specifications in Figure 2).

For the generation of the RESOURCECODE wave data base, 3 parameters from the ST4 source term packages have been tuned to optimize WW3 performance with the set of forcing fields used (see section 2.3). The maximum value of the wind-wave coupling β_{max} (BETAMAX) was set to 1.75, the swell dissipation factor SWELLF7 was set to 432000 and the Reynolds number critical value SWELLF4 was set to 115000. In addition, an 5% boost to winds higher that 21 [m/s] was applied to improve the negative bias of high winds from the input source, this correction is done using the WCOR1 and WCOR2 variables. The complete list of parameters is shown in Figure 3.

```
&SPECTRUM_NML
  SPECTRUM%XFR       =  1.1     ! frequency increment
  SPECTRUM%FREQ1     =  0.0339  ! first frequency (Hz)
  SPECTRUM%NK        =  36      ! number of frequencies (wavenumbers)
  SPECTRUM%NTH       =  36      ! number of direction bins
/
```

Figure 1 : Model spectral discretization

Obs.: parameters included in ww3_grid.nml file.

```
&TIMESTEPS_NML
  TIMESTEPS%DTMAX        =  180.   ! maximum global time step (s)
  TIMESTEPS%DTXY         =  30.    ! maximum CFL time step for x-y (s)
  TIMESTEPS%DTKTH        =  15.    ! maximum CFL time step for k-th (s)
  TIMESTEPS%DTMIN        =  5.     ! minimum source term time step (s)
/
```

Figure 2 : Time steps' specifications

Obs.: parameters included in ww3_grid.nml file.

```
&SIN4 BETAMAX = 1.75, SWELLF = 0.66, TAUWSHELTER = 0.3,
      SWELLF3 = 0.022,  SWELLF4 = 115000.0, SWELLF7 = 432000.00 /

&SDS4 FXFM3 = 2.5 /

&PRO3 WDTHCG = 1.50, WDTHTH = 1.50  /

&SIC2 IC2DISPER = F, IC2TURB = 1.0, IC2ROUGH = 0.001, IC2DMAX = 0.3,
      IC2REYNOLDS = 150000, IC2SMOOTH = 200000., IC2VISC = 2. /

&SIS2 ISC1 = 0.2, IS2C2 = 0., IS2C3 = 0., IS2BACKSCAT = 1.,
      IS2BREAK = T, IS2DUPDATE = F, IS2CREEPB = 0.2E8, IS2CREEPD = 0.5,
      IS2CREEPN = 3.0, IS2BREAKE = 1.0, IS2BREAKF = 3.6, IS2WIM1 = 1.0,
      IS2FLEXSTR = 2.7414E+05, IS2CREEPC = 0.4,
      IS2ANDISB = T, IS2ANDISD = 0.2E-8, IS2ANDISE = 0.55, IS2ANDISN = 1.0 /

&REF1 REFCOAST = 0.05, REFCOSP_STRAIGHT = 4, REFFREQ = 1., REFICEBERG = 0.2,
      REFMAP = 0., REFSLOPE = 0., REFSUBGRID = 0.1, REFRMAX = 0.5 /

&MISC NOSW = 6, WCOR1 = 21., WCOR2 = 1.05 /

&OUTS E3D = 1 /

&UNST UGBCCFL = F, UGOBCAUTO = T, UGOBCDEPTH = -15.0, EXPFSN = T/

&SBT4 SEDMAPD50 = T, BOTROUGHMIN =  0.0400, BOTROUGHFAC = 1.0 /

END OF NAMELISTS
```

Figure 3 : Physical parameters' specification

Obs.: parameters included in namelist.nml file.

2.3 Forcing fields and boundary conditions

The model was forced using ERA5 wind fields, and tidal levels and currents generated with astronomic harmonics. In addition, a detailed D50 sediment map was used to take into account bottom induced wave dissipation during propagation in intermediate waters. Details on the sea bottom sediment types is further explained in section 2.5.

2.3.1 Wind fields

The used ERA5 wind data (https://doi.org/10.24381/cds.adbb2d47), extends from 1979 to 2020. U and V intensities, defined at a 10 [m] height above the sea surface, are distributed over a 0.25° (~30 [km]) grid. The original wind fields' geographical domain is defined within 0° to 359.75° longitude, and -90° to 90° latitude. The wind intensity's fields are presented hourly (which means that the wind forcing is also updated hourly).

For more details:

https://confluence.ecmwf.int/display/CKB/ERA5+data+documentation

2.3.2 Tidal levels and currents

Tidal levels and currents within the modelled domain were reconstructed from tidal harmonics M2 S2 N2 using **ww3_prtide**. Those tidal harmonics were

processed based on the amplitudes and phases from a total of 14 constituents that were employed: O1, P1, K1, N2, M2, S2, K2, MN4, M4, MS4, M6 Mf, and Mm. This method is based on the Versatile Harmonic Tidal Analysis by Foreman et al. 2009.

The set of harmonics were taken from 2 different sources. The first one, is the output from the tidal atlas generated at Ifremer using the MARS 2D (Lazure & Dumas; 2008) hydrodynamic model, based on the shallow water equations. A total of 5 grids with 3 levels of nesting, and having different spatial resolution were selected. The lowest nesting level 0 corresponds to the largest modelled domain where all the other sub-models are nested. The details of the selected models from Ifremer's tidal atlas are presented in Table 1.

The second tidal data source was used to cover part the coast of Portugal in the Atlantic and up to the eastern end of the Gibraltar straight (which are not included in Ifremer's tidal atlas), The data was taken from the native mesh of the FES2014[1] model, re-grided to 0.004° (~450 [m]).

The tidal data from both sources was merged and interpolated into the unstructured mesh nodes (see Figure 5). To avoid discontinuities at the boundaries between the merged models, a gap of 0.1° was introduced before the interpolation (see Figure 4). In those areas where no data was available, the nearest neighbor extrapolation was applied. A clear example of the latter case is the eastern end of the Bristol Channel, but in general extrapolation was done in very shallow coastal areas over short distances.

The tidal level and currents are updated every 30minutes on each node of the mesh.

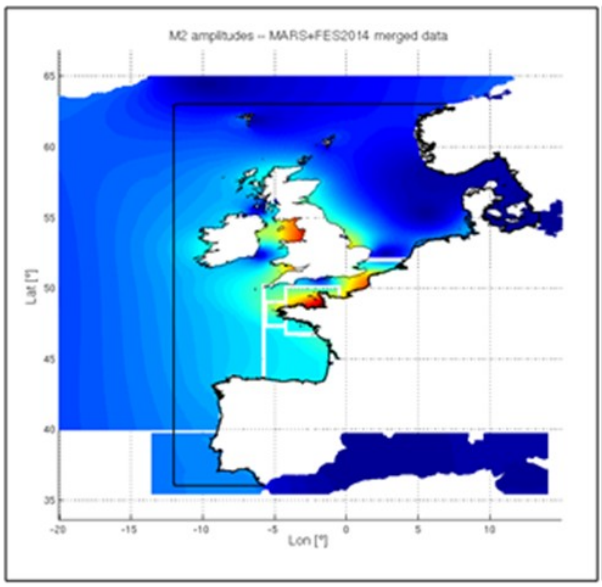

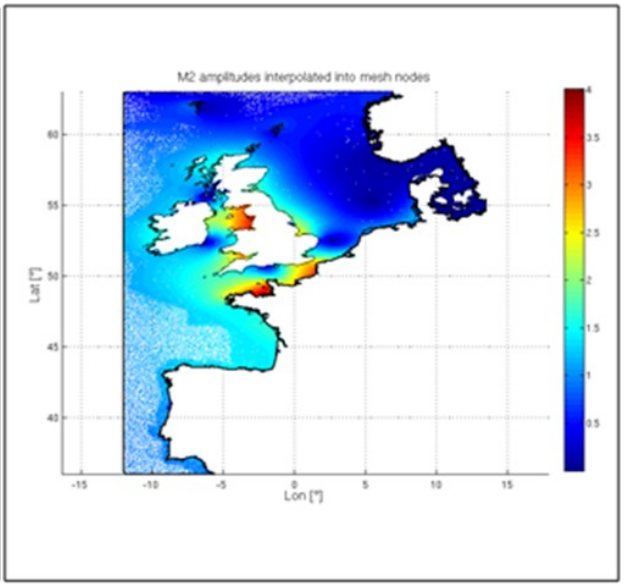

Figure 4 : (on the left) M2 amplitudes from Ifremer's tidal atlas models and FES2014

Figure 5 : (on the right) Merged tidal data interpolated into RESOURCECODE unstructured mesh nodes

Obs.: Colorbar represents tidal amplitudes in meters. Outer thick black line denotes the boundary of the model, while black thin lines are the internal coastlines.

Table 1 : Models selected from Ifremer's tidal atlas

Nesting Level	Spatial resolution [m]	Model domain limits		Region	Model Name
		Longitude [°]	Latitude [°]		
0	2000	-20.03 to 14.98	39.98 to 64.98	Atlantique Nord Est	ATLNE2000
1	700	-5.73 to 4.18	43.28 to 52.00	Manche et Golfe de Gascogne	MANGA700
2	250	-5.63 to -3.66	47.34 to 49.03	Mer de Iroise	FINIS250
2	250	-4.23 to -1.96	46.78 to 47.93	Bretagne Sud	SUDBZH250
2	250	-4.21 to -0.50	48.45 to 50.10	Manche Ouest	MANW250

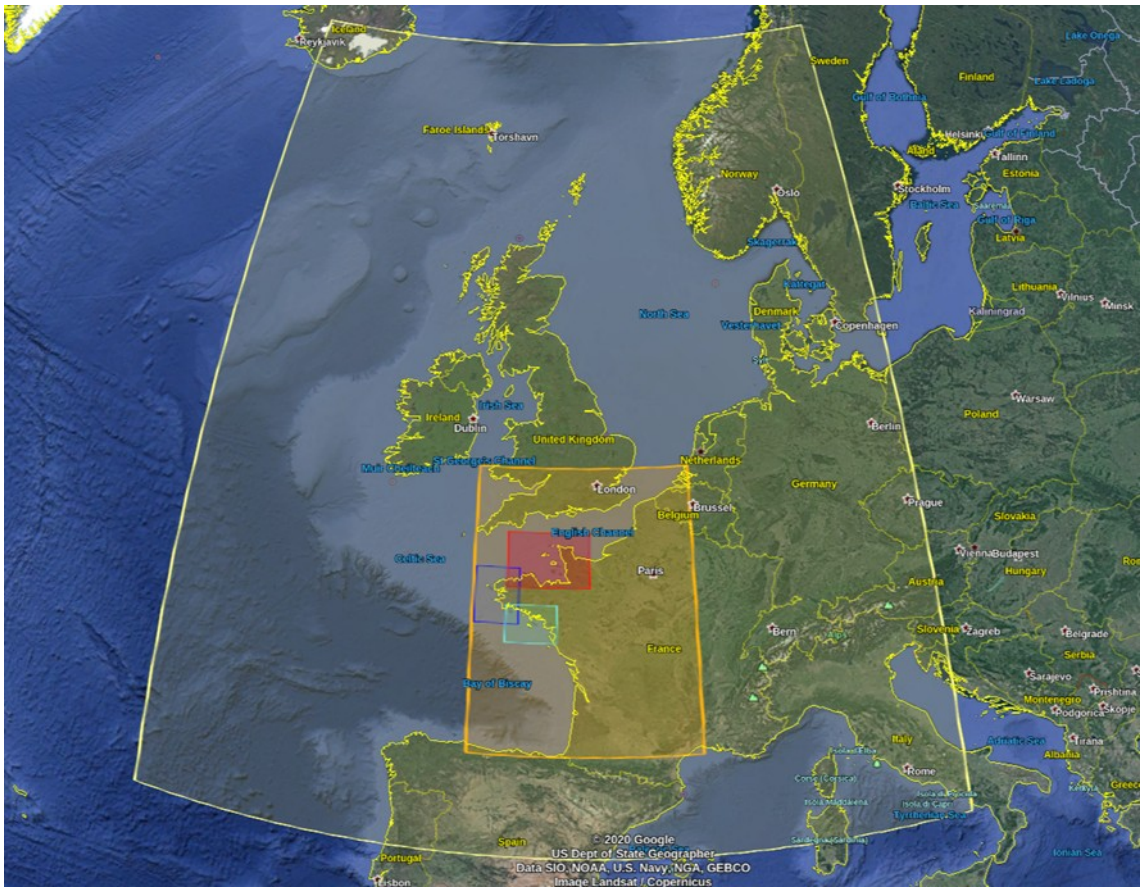

Figure 6 : Ifremer's tidal atlas

Obs.: Blue rectangle shows the area of FINIS250 model, Light blue rectangle shows the area of SUDBZH250, and red rectangle shows the area of MANW250.

Image source: Google Earth.

2.3.3 Boundary conditions

Boundary conditions were taken from a global hindcast generated with the same parametrizations and spectral discretization as those specified in sections 2.1 and 2.2, and on a 0.5° resolution regular grid. This global model was forced with ERA5 winds and CMEMS GlobCurrent Total surface currents (integrated geostrophic and Ekman components). The results of the global hindcast were analyzed and validated at LOPS, as part of the CCI Sea State project.

A total number of 104 nodes along the southern, western and northern boundaries of the mesh were used to prescribe the (directional) spectral boundary conditions (see Figure 7). It should be specified that the boundary conditions are interpolated in space into each active boundary node of the

mesh, and in time to provide directional spectral data each hour, since the global model provides output only with a 3-hour time step.

Figure 7 : Nodes with directional spectra used to set boundary conditions in mesh nesting

Obs : Red dots specify the position of the spectral data from the global grid requested to nest the RESOURCECODE mesh

Image source: Google Earth.

2.4 Bathymetry and coastlines

2.4.1 Bathymetry sources

Two bathymetry sources were integrated into a xyz-type file which was used as input for the mesh generation. The data sources are the following:

EMODnet: Depth terrain model (DTM, 2016 version) which integrates several surveys along the French coast, the North Sea and the North Atlantic (high latitudes included) from 41 partners, including SHOM as leading partner. The

available data has a resolution of 0.0021° (1/8 arc minutes, ~210 [m]), the depth reference system is the Lowest Astronomical Tide (LAT) and the geographic coordinates' system is WGS-84. Data coverage includes the complete model domain (see Figure 8). For details, please go to: http://portal.emodnet-bathymetry.eu/ .

HOMONIM: DTM provided by SHOM (https://data.shom.fr)[2]. The DTM resolution is 0.001° (~ 111 m) and the geographic coordinates' system is WGS-84. The depth reference selected is LAT. Data coverage is smaller than the model domain required for RESOURCECODE (HOMONIM model domain: Lon: [-6° 5.85°], Lat: [43.25° 52.9°]; see Figure 9).

When merging the datasets, the EMODnet data in areas covered by the HOMONIM DTM were replaced by this latter to increase resolution in these areas. The merged bathymetric data, used in the mesh generation is presented in Figure 10.

Bathymetry data input in WW3 must be defined with respect to the Mid Sea Level (MSL), therefore a correction was applied to the depths defined with respect LAT. According to the IHO (International Hydrographic Organization) a relation between the MSL and the LAT can be obtained using the harmonic constants derived from the analysis of previous observations. In this case, the harmonic constants were taken from the FES model output (2014). The generic expression that relates LAT and MSL is of the form:

LAT = Z0 - (M2 + S2 + N2 + K1 + O1 + …)

where: Z0 : mean sea level.

M2, S2, N2, K1, O1, etc.. : Harmonic components' amplitudes.

After a sensitivity analysis, 10 harmonics were used in the previous expression to change the depth datum into MSL: O1, K1, M2, S1, N2, K2, M4, MS4, MN4, M6. The sensitivity analysis was done to reduce the differences between the HOMONIM dataset with respect to MSL, and the HOMONIM dataset with respect to LAT transformed into MSL. It was verified that with the 10 selected harmonics, the largest differences where of the order of -15% to +15% in very shallow areas (see Figure 11).

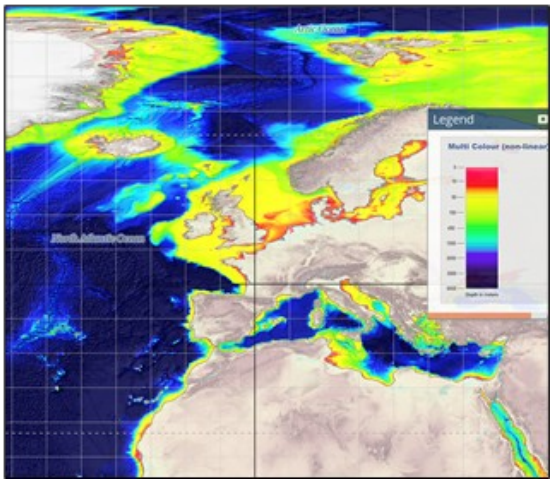

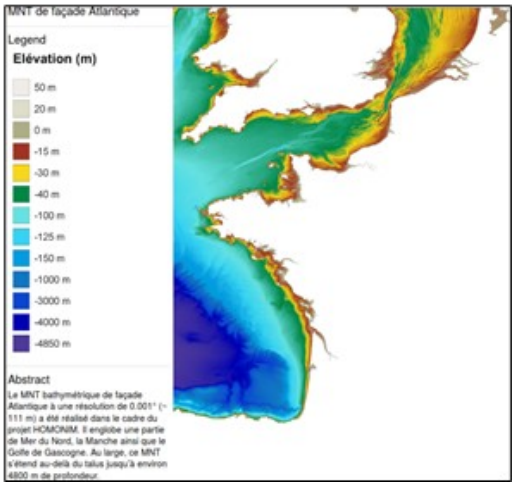

Figure 8 : (on the left) Example of data coverage from EMODnet DTM

Figure 9 : (on the right) Data coverage from HOMONIM DTM

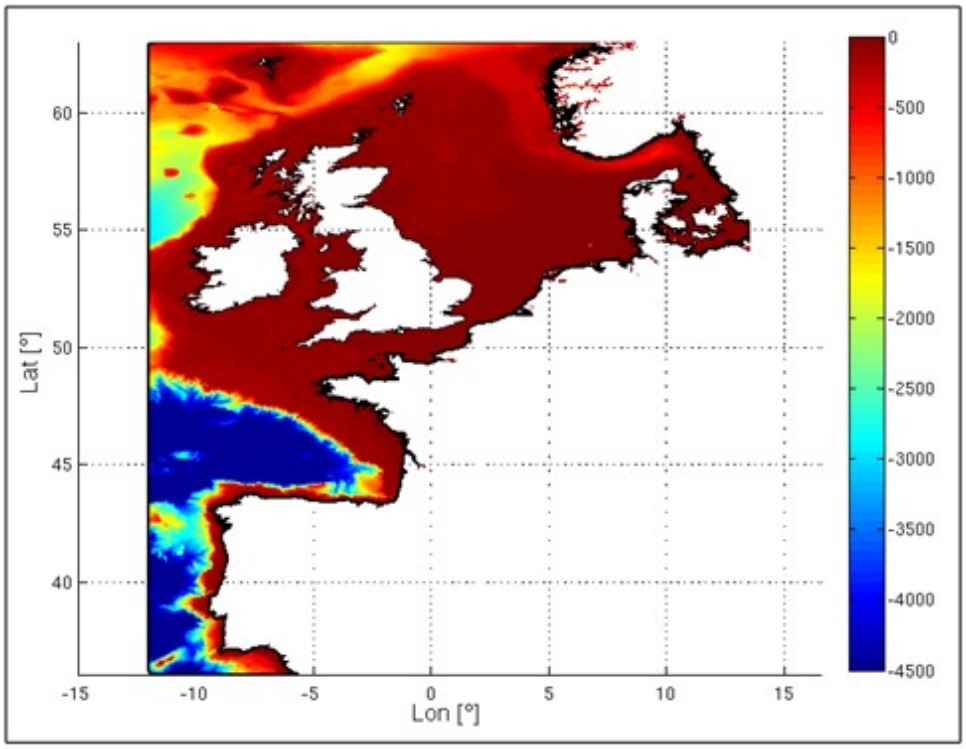

Figure 10 : Bathymetry data (w/r to MSL) used in mesh generation

Obs.: Colorbar represents depth values with respect to MSL in meters. Outer thick black line denotes the boundary of the model, while black thin lines are the internal coastlines.

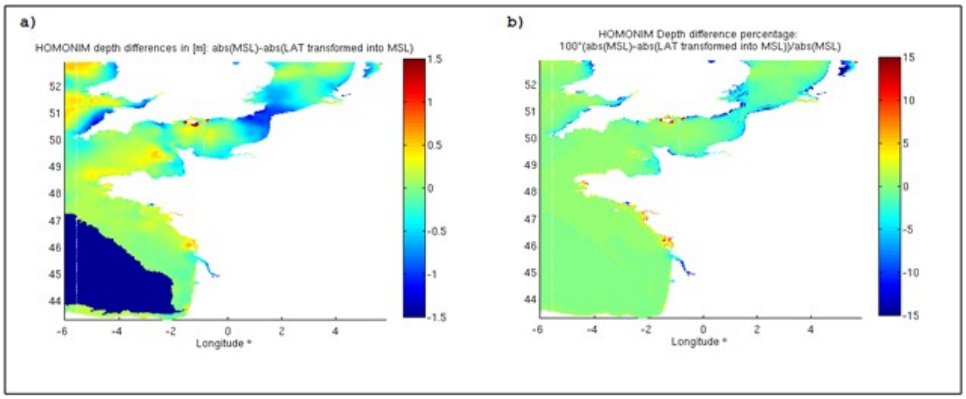

Figure 11 : Depth differences in HOMONIM MSL v/s HOMONIM transformed from LAT to MSL

Left image: Absolute depth difference between HOMONIM MSL and HOMONIM in LAT transformed into MSL. Right image: Relative depth difference between HOMONIM MSL and HOMONIM in LAT transformed into MSL.

Obs.: Larger depth differences in deep areas between 44° and 47° latitude, is due to no tide correction in HOMONIM dataset provided in MSL.

2.4.2 Coastline source

All coastlines utilized in the mesh generation were taken from OpenStreetMap polygons:

Projection: WGS-84

Last update of used data set: 2018-06-10 09:33.

Source: http://openstreetmapdata.com/data/land-polygons

These polygons define the mean high-water spring, which means that their elevation should be placed above sea mean waver level according to local tide conditions, although source files only have longitude and latitude information, no elevation is provided. For the case of the RESOURCECODE regional model, all coastlines' vertical coordinates were set to 2 [m] depth to avoid unrealistic wave height (Hs) gradients in extremely shallow water conditions, and to prevent excessive dry nodes effect in the mesh due to tidal levels variations. This consideration is especially important in areas with large tide coefficients.

Due to the uneven distribution of nodes within the polygons, a homogenization was applied. The average resolution at the coast after segments' splitting (in the mesh generation process) is about ~200 to ~300 [m]. Extra coarsening, up to 1200 [m], removal of islands, and sections' trimming were applied at the fjords along the Norwegian coast to simplify this area (which is out of the scope of the present project).

The final set of polygons are presented in Figure 12 (also in Figure 10 in context with the bathymetric data), and in Figure 13 is possible to see the areas left out of the model due to trimming and coarsening of coastline polygons along the Norwegian fjords.

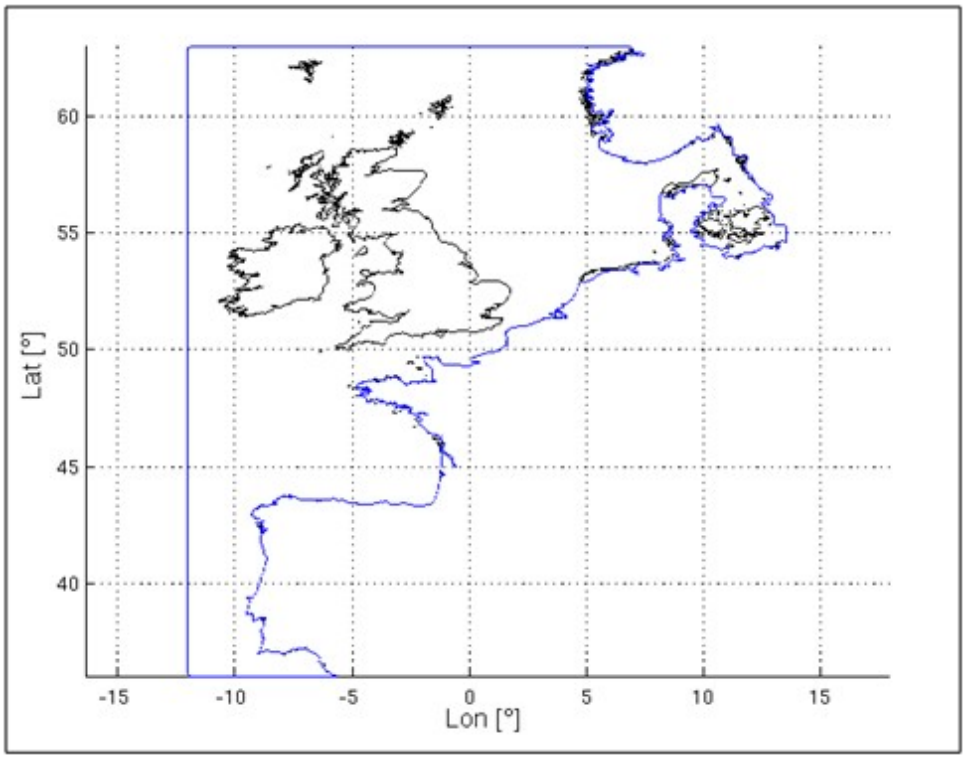

Figure 12 : Coastline polygons and boundary polygon

Obs.: Blue line denotes the mesh boundary polygon. Black line shows coastlines inside the model domain.

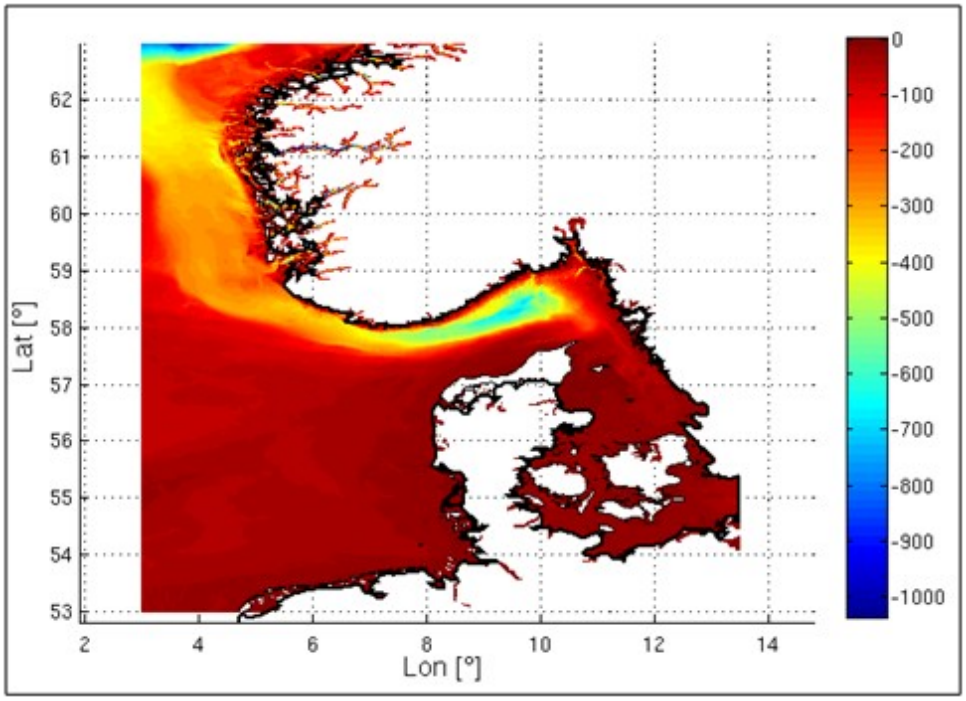

Figure 13 : of modified coastline (trimmed polygons) along Norwegian coastline

Obs.: Colorbar represents depth values with respect to MSL in meters. Outer thick black line denotes the boundary of the model, while black thin lines are the internal coastlines.

2.5 Sediment types sources used for bottom friction

Bottom sediment types are characterized by its D50 diameter in meters. The D50 values are used as input in the BT4 parametrization for dissipation due to bottom friction (explained in section 2.1).

Two sources of sediment classifications were used in the construction of the sediment D50 map. The first source of sea bottom substrate classification was obtained from the EMODnet database (http://www.emodnet-geology.eu/data-products/). Specifically, the Seabed Substrate map 1:1M shape files, which extension covers the complete RESOURCECODE mesh domain. In addition, bottom sediment classes from SHOM, along the French Atlantic coast and along La Manche channel, were merged to the previous dataset to obtain a more detailed sediment type distribution in these areas. It must be highlighted that the SHOM sediment database was previously used for the HOMERE project which allows to use with confidence the correspondences for the sediment classifications to a given averaged grain size D50. Some reference D50 values from the previous mesh NORGAS-UG were taken into account in the generation

of the new sediment map for the RESOURCECODE mesh. More details about the SHOM sediment product can be found at:

https://diffusion.shom.fr/pro/ressources/sedimentologie.html

To create the bottom sediment map, an averaged D50 value (in meters) was associated to each sediment class, and since 2 different sources with different classification systems were employed, special attention was paid to keep a consistent D50 values distributions. The final sediment D50 values assigned to each node of the mesh are provided in the **RSCD-UG.SED50.dat** file. These final values were defined after a sensitivity analysis and corresponding buoy validation process (see Figure 14 and 15).

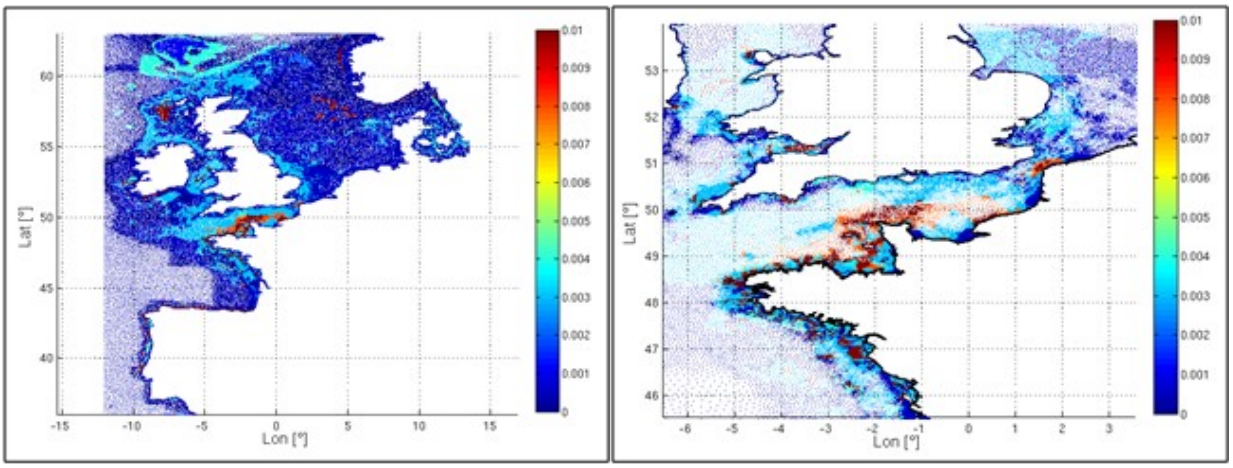

Figure 14 : (on the left) D50 distribution in complete mesh

Figure 15 : (on the right) Detail of D50 distribution in The Channel and Brittany coast

Obs.: Colorbar represents D50 diameter in meters. Max value in colorbar has been selected to enhance visualization of different sediment types visualization.

2.6 Mesh generation generalities

The RESOURCECODE mesh was generated using Polymesh 2-D Mesh Generator, developed at BGS IT&E. Nodes from the NORGAS-UG mesh (HOMERE project) were included in the new mesh, except for those placed less than 800 [m] away from the coastlines. This was done to keep, as much as possible, the already well accomplished refined areas and numerical stability conditions from the NORGAS-UG mesh within this area of the modelled domain.

Special refinement conditions were applied in 14 different sites following specifications of the project's partners. These areas are mainly renewable energy test sites or project sites, with the exception of the refinement applied in the southern part of the North Sea, which was included to have a better

representation of the complex bottom morphology features in this area. The set of polygons used to define the sections where special mesh refinement was required, are presented in Figure 16 along with an example of the obtained mesh's nodes distribution (see Figure 17).

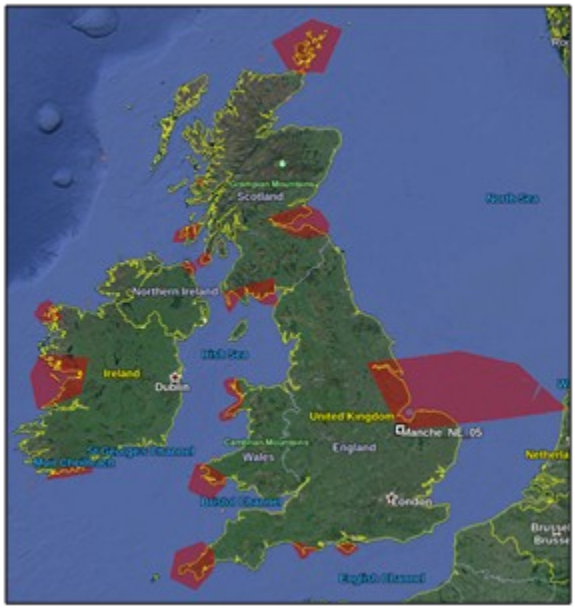

Figure 16 : Distribution of refinement polygons used in Polymesh

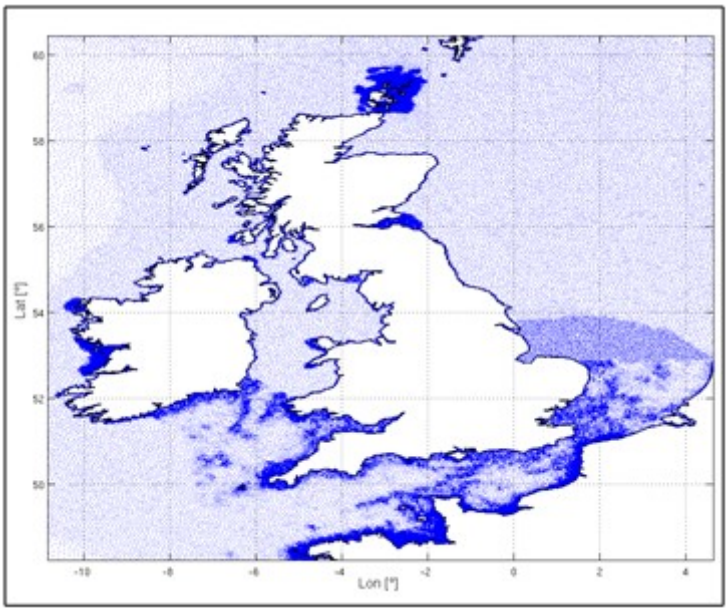

Figure 17 : Detail of node distribution in areas where special refinement was applied

Obs.: Refinement polygons presented in red in left image.

Left image source: Google Earth.

3 Database organization and description

3.1 File formats

The products are provided in netCDF4 format, which is a binary file format widely used in the scientific community. Each file contains a header with a description of the data and the metadata. Users must pay attention to the attributes associated with each variable described in the netcdf file to correctly handle the data. By default, matlab and python functions used for netcdf file reading, automatically apply the "_FillValue", "scale_factor" and "add_offset" attributes on the data:

```
Variable.data = Where (Variable.data != Variable._FillValue)
                    { (Variable.data * Variable.scale_factor) + Variable.add_offset }
```

3.2 File tree organization

Accessing to the dataset through the ftp repository, the file tree is organized by year, then by month. The content of each monthly directory is detailed in Table 2.

Table 2 : dataset organization

wavesetup.env	Environment file used for the run
FIELD_NC	Field output files (see section 4.1)
SPEC_NC	Directional spectra files (see section 4.2)
FREQ_NC	Frequency spectra files (see section 4.3)
Data	configuration files for the grid and some template files
Work	All the configuration files used for the run
Output	All the log files generated during the run
STATION	Comparison with CMEMS InSituTAC buoys
SAT	Comparison with CCI Sea State V1 altimeters

4 Output parameters

4.1 Field output

Global integral parameters NetCDF files inside the **FIELD_NC** folders have the following name structures:

RSCD_WW3-RSCD-UG-**YYYYMM**.nc

RSCD_WW3-RSCD-UG-**YYYYMM_wn**.nc

RSCD_WW3-RSCD-UG-**YYYYMM_ef**.nc

The main variables contained in these files are described in Table 3, 4 and 5 respectively. The grid is described as a triangle-based mesh where all the triangles' vertex are named as node. Each node location is provided according to latitude and longitude coordinates. Each triangle can be reconstructed with its 3 vertices, named here as element. Each value of the element represents the index of a node in the mesh. For wave number and frequency spectrum, the frequency is the central frequency of each frequency bin used to integrate the wave spectrum. For the complete list of parameters and their description, please verify the full list of variables in the respective files.

Table 3 : Output variables in global integral parameters files

Variable	Variable name in file	Units	Comment
Depth	**dpt**	[m]	positive downward
Eastward current	**ucur**	[m s-1]	cur=sqrt(ucur**2+vcur**2)
Northward current	**vcur**	[m s-1]	cur=sqrt(ucur**2+vcur**2)
Eastward wind	**uwnd**	[m s-1]	wind=sqrt(uwnd**2+vwnd**2)
Northward wind	**vwnd**	[m s-1]	wind=sqrt(uwnd**2+vwnd**2)
Sea surface height above sea level	**wlv**	[m]	
Sediment grain size	**d50**	[Krumbein phi scale]	
Significant wave height	**hs**	[m]	height of wind and swell waves
Mean wave length	**lm**	[m]	
Mean period T02	**t02**	[s]	from second frequency moment

Mean period T0m1	**t0m1**	[s]	from inverse frequency moment
Mean period T01	**t01**	[s]	from first frequency moment
Wave peak frequency	**fp**	[s-1]	
Wave mean direction	**dir**	[degree]	comes from
Directional spread	**spr**	[degree]	
Mean direction at peak frequency	**dp**	[degree]	comes from
Significant wave height of partitions	**phs[0-5]**	[m]	defined using topographic partitions and partition wave-age cut-off, ordered as: 0: wind-sea 1: most energetic swell 2: second most energetic swell 3: third most energetic swell 4: fourth most energetic swell 5: fifth most energetic swell
Peak period of partitions	**ptp[0-5]**	[s]	“
Peak wave length of partitions	**plp[0-5]**	[m]	“
Wave mean direction of partitions	**pdir[0-5]**	[degree]	comes from
Directional spread of partitions	**pspr[0-5]**	[degree]	“
Wind sea fraction in partitions	**pws[0-5]**	[1]	“
Mean direction at peak frequency of partitions	**pdp[0-5]**	[degree]	comes from
Wind sea fraction	**tws**	[1]	defined using topographic partitions and partition wave-age cut-off
Eastward friction velocity	**uust**	[m s-1]	ust=sqrt(uust**2+vust**2)
Northward friction velocity	**vust**	[m s-1]	ust=sqrt(uust**2+vust**2)
Charnock coefficient for surface roughness length for momentum in air	**cha**	[1]	
Wave energy flux	**cge**	[kW m-1]	

Wind to wave energy flux	**faw**	[W m-2]	
Eastward wave supported wind stress	**utaw**	[m2 s-2]	taw=sqrt(utaw**2+vtaw**2)
Northward wave supported wind stress	**vtaw**	[m2 s-2]	taw=sqrt(utaw**2+vtaw**2)
Eastward wave to wind stress	**utwa**	[m2 s-2]	twa=sqrt(utwa**2+vtwa**2)
Northward wave to wind stress	**vtwa**	[m2 s-2]	twa=sqrt(utwa**2+vtwa**2)
Whitecap coverage	**wcc**	[1]	
Eastward wave to ocean stress	**utwo**	[m2 s-2]	two=sqrt(utwo**2+vtwo**2)
Northward wave to ocean stress	**vtwo**	[m2 s-2]	two=sqrt(utwo**2+vtwo**2)
Wave to ocean energy flux	**foc**	[W m-2]	
Eastward stokes transport	**utus**	[m2 s-1]	tus=sqrt(utus**2+vtus**2)
Nnorthward stokes transport	**vtus**	[m2 s-1]	tus=sqrt(utus**2+vtus**2)
Eastward surface stokes drift	**uuss**	[m s-1]	uss=sqrt(uuss**2+vuss**2)
Northward surface stokes drift	**vuss**	[m s-1]	uss=sqrt(uuss**2+vuss**2)
Rms of bottom displacement amplitude zonal	**uabr**	[m]	abr=sqrt(uabr**2+vabr**2)
Rms of bottom displacement amplitude meridional	**vabr**	[m]	abr=sqrt(uabr**2+vabr**2)
Rms of bottom velocity amplitude zonal	**uubr**	[m s-1]	ubr=sqrt(uubr**2+vubr**2)
Rms of bottom velocity amplitude meridional	**vubr**	[m s-1]	ubr=sqrt(uubr**2+vubr**2)
Downwave mean square slope	**mssu**	[1]	
Crosswave mean square slope	**mssc**	[1]	
Mean square slope direction	**mssd**	[degree]	
Map status	**MAPSTA**	n/a	0=sea, 1=land, 2=open boundary, 3=excluded
Triangle id	**tri**	n/a	Expressed by 3 vertices, named element which are node index

Time	**time**	[days]	days since 1990-01-01 00:00:00Z
Longitude	**longitude**	[degrees east]	range from –180 to 180
Latitude	**latitude**	[degrees north]	range from –90 to 90

Table 4 : Output variables in wave number files

Variable	Variable name in file	Units	Comment
Wave number	**wn**	[m-1]	
Map status	**MAPSTA**	n/a	0=sea, 1=land, 2=open boundary, 3=excluded
Triangle id	**tri**	n/a	Expressed by 3 vertices, named element which are node index
Time	**time**	[days]	days since 1990-01-01 00:00:00Z
Longitude	**longitude**	[degrees east]	range from –180 to 180
Latitude	**latitude**	[degrees north]	range from –90 to 90
Wave frequency	**f**	[s-1]	central wave frequency

Table 5 : Output variables in wave elevation spectrum files

Variable	Variable name in file	Units	Comment
Wave elevation spectrum	**ef**	[log10(m2 s+1E-12)]	where (ef != _FillValue) ef=pow(10, ef*scale_factor)-1E-12
Map status	**MAPSTA**	n/a	0=sea, 1=land, 2=open boundary, 3=excluded
Triangle id	**tri**	n/a	Expressed by 3 vertices, named element which are node index
Time	**time**	[days]	days since 1990-01-01 00:00:00Z
Longitude	**longitude**	[degrees east]	range from –180 to 180

Latitude	**latitude**	[degrees north]	range from –90 to 90
Wave frequency	**f**	[s-1]	central wave frequency

4.2 Directional spectra output

Directional spectra NetCDF files inside the **SPEC_NC** folders have the following name structure:

RSCD_WW3-RSCD-UG-**NodeID**_**YYYYMM**_**spec**.nc

The main variables contained in these files are described in Table 6. The lower, central and higher frequency values are related to the frequency bins used for integration of the spectrum. For the complete list of parameters and their description, please verify the full list of variables in the respective files.

It must be noticed that the direction bins array is stored with first index at 90 (East), then going counterclockwise, meaning [90; 80; 70; 60; ...10; 0; 350; 340; ...270; 260; ...; 110; 100]

Table 6 : Output variables in directional spectra files

Variable	Variable name in file	Units	Comment
Lower frequency	**frequency1**	[s^{-1}]	df=frequency2-frequency1
Central frequency	**frequency**	[s^{-1}]	Exponentially spaced by factor 1.1
Higher frequency	**frequency2**	[s^{-1}]	df=frequency2-frequency1
Direction	**Direction**	[degree]	going to
Surface elevation variance spectral density	**efth**	[log10(m^2 s rad^{-1} + E-12)]	where (efth != _FillValue) efth=pow(10, efth*scale_factor)-1E-12
Depth	**dpt**	[m]	positive downward
Wind intensity	**wnd**	[m s^{-1}]	at 10 [m] above sea level
Wind direction	**wnddir**	[degree]	comes from

Current intensity	**cur**	[m s^{-1}]	at the surface
Current direction	**curdir**	[degree]	comes from
Time	**time**	[days]	days since 1990-01-01 00:00:00Z
Longitude	**longitude**	[degrees east]	range from –180 to 180
Latitude	**latitude**	[degrees north]	range from –90 to 90
Station id	**station**	n/a	value between 1 and 24162
Station name length	**string40**	n/a	empty
Station name	**station_name**	n/a	name stored on 40 characters

4.3 Frequency spectra output

Frequency spectra data files are contained inside the **FREQ_NC** folders. The files' name structure is as follows:

RSCD_WW3-RSCD-UG-**NodeID**_**YYYYMM**_**freq**.nc

Main variables included in these files are listed in Table 7. The 1D frequency spectral are obtained from the directional spectral files by integrating the data in the directional space. As for the previous case, the lower, central and higher frequency values, are related to the frequency bins used for integration of the spectrum.

Table 7 : Output variables in frequency spectra files

Variable	Variable name in file	Units	Comment
Lower frequency	**frequency1**	[s^{-1}]	df=frequency2-frequency1
Central frequency	**frequency**	[s^{-1}]	Exponentially spaced by factor 1.1
Higher frequency	**frequency2**	[s^{-1}]	df=frequency2-frequency1
Surface elevation variance spectral density	**ef**	[m^2 s]	
Mean direction from first spectral moment	**th1m**	[degree]	

Mean direction from second spectral moment	**th2m**	[degree]	
Mean directional spreading from first spectral moment	**sth1m**	[degree]	
Mean directional spreading from second spectral moment	**sth2m**	[degree]	
Depth	**dpt**	[m]	positive downward
Wind intensity	**wnd**	[m s^{-1}]	at 10 [m] above sea level
Wind direction	**wnddir**	[degree]	comes from
Current intensity	**cur**	[m s^{-1}]	at the surface
Current direction	**curdir**	[degree]	going to
Significant wave height	**hs**	[m]	
Peak wave frequency	**fp**	[s^{-1}]	
Mean wave frequency	**f02**	[s^{-1}]	from second spectral moment
Mean wave frequency at spectral moment minus one	**f0m1**	[s^{-1}]	from inverse spectral moment
Mean wave direction at spectral peak	**th1p**	[degree]	comes from
Directional spreading at spectral peak	**sth1p**	[degree]	
Mean wave direction	**dir**	[degree]	comes from
Mean directional spreading	**spr**	[degree]	
Time	**time**	[days]	days since 1990-01-01 00:00:00Z
Longitude	**longitude**	[degrees east]	range from –180 to 180
Latitude	**latitude**	[degrees north]	range from –90 to 90
Station id	**station**	n/a	value between 1 and 24162

Station name length	**string40**	n/a	empty
Station name	**station_name**	n/a	name stored on 40 characters

5 Validation

To fully assess the model performance, an extensive validation work was conducted based on the derivation of statistical error estimators established comparing the model data with wave buoys and remote sensing data. Reference parameter used for this validation was mainly the significant wave height. However, spectral validation over frequencies following the methodology proposed by Perignon 2017 and applied for the assessment of the HOMERE database (Perignon2017b) was also conducted at locations where wave spectra derived from wave buoys were available.

The normalized bias (NB), normalized root mean square difference (NRMSE), scatter index (SI) and correlation coefficient (R) are employed as performance estimators.

$$NB(X) = \frac{\sum(Xmod - Xobs)}{\sum Xobs}$$

$$NRMSE(X) = \sqrt{\frac{\sum (Xmod - Xobs)^2}{\sum Xobs^2}}$$

$$SI(X) = \sqrt{\frac{\sum[(Xmod - \overline{Xmod}) - (Xobs - \overline{Xobs})]^2}{\sum Xobs^2}}$$

$$R(X) = \frac{\sum(Xmod - \overline{Xmod})(Xobs - \overline{Xobs})}{\sqrt{\sum (Xmod - \overline{Xmod})^2 \sum (Xobs - \overline{Xobs})^2}}$$

With X for any quantity of modeled data (Xmod) and observation data (Xobs). The overbar denotes the arithmetic average.

5.1 Altimeter Data

The sea surface significant wave height estimated by the altimeter database from the CCI Sea State V1 for the period 1994-2018 was used. It offers a good consistency in space and time to assess the overall model performance. The studied area is covered by all the altimeters provided except Cryosat-2 which is in SAR mode in the North-East Atlantic. Due to issues on the onboard

instrumentations, ERS-1 data after 1995 and ERS-2 data after 2002 were not used. Data from currently working satellites Saral and Jason-2 were not yet available for 2019 and 2020 in this version.

The methodology applied for this model validation was to obtain matches-up of the model output along each altimeter track by performing a spatio-temporal interpolation. Altimeters' data considered unreliable (tracks within 50km from coasts, significant wave height lesser than 1m and affected by noise) were disregarded. A merged product was then generated by gathering all the altimeters data available to produce yearly analysis (see Figure 18).

Overall statistics presented in table 8 indicate a good agreement between model and altimeter data for all altimeters which allow us to assess the overall model performances for the significant wave height with really encouraging scores on the merged satellite product from 1994 to 2018. The normalized bias is 0.26% (0.7cm) with a NRMSE at 10.30% (30.7cm). The scatter index is very similar to the NRMSE which shows a limited impact of the bias on the random error. The correlation coefficient is steady around 97%.

Table 8 : Overall statistics per altimeter

Satellite	Covered period	B (m)	NB (%)	RMSE (m)	NRMSE (%)	SI (%)	R (%)
ERS-1	1994-1995	0.021	1.20	0.300	10.61	9.05	93.87
TOPEX	1994-2005	-0.013	-0.32	0.325	10.52	10.16	97.11
ERS-2	1995-2002	0.004	0.23	0.308	10.73	10.03	96.08
GFO	2000-2008	0.008	0.44	0.315	10.37	9.85	96.96
JASON-1	2002-2013	0.001	0.04	0.307	10.06	9.56	96.90
ENVISAT	2002-2012	0.011	0.47	0.292	9.86	9.06	96.11
JASON-2	2008-2018	0.011	0.28	0.308	10.08	9.56	96.92
SARAL	2013-2018	0.015	0.47	0.279	9.42	8.64	97.03
JASON-3	2016-2018	0.014	0.37	0.292	10.14	9.78	97.16
MERGED	1994-2018	0.007	0.26	0.307	10.30	9.82	96.80

The time series of the statistical estimators (see Figure 18) reveal a good correlation over years with a trend to better scores and lower fluctuations in recent years. The important point is to demonstrate that model performances are steady over the covered period with less than 2% of variation for the SI, NRMSE and NB.

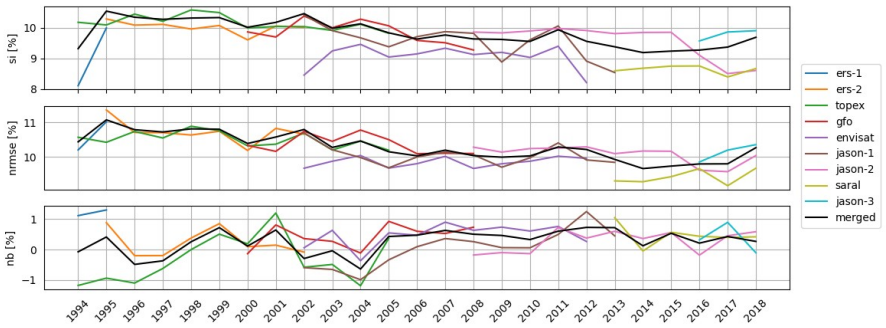

Figure 18: Overall time series of SI, NRMSE and NB

The along-track data were averaged over a regular 1/8° grid to allow further yearly estimates (see Figure 19).

The benefit of the altimeter global coverage is to supply a map of significant wave height with a sufficient amount of yearly matches-up (Fig. 19c) to compute reliable estimates (Fig. 19d) on the whole domain. The NB (Fig. 19a) and NRMSE (Fig. 19b) reveal some interesting patterns which worth further investigation. The Scottish Sea has a positive bias associated with a higher random error. The South-West of the North Sea has a lower correlation coefficient related to a negative bias and a stronger RMSE. On average, NB tends to be positive in the Atlantic Ocean and negative in the North Sea. The NRMSE and NB increase in shallow water and sheltered areas.

Those discrepancies can be due to both altimeters' errors, model parameterization and wind and current forcing fields.

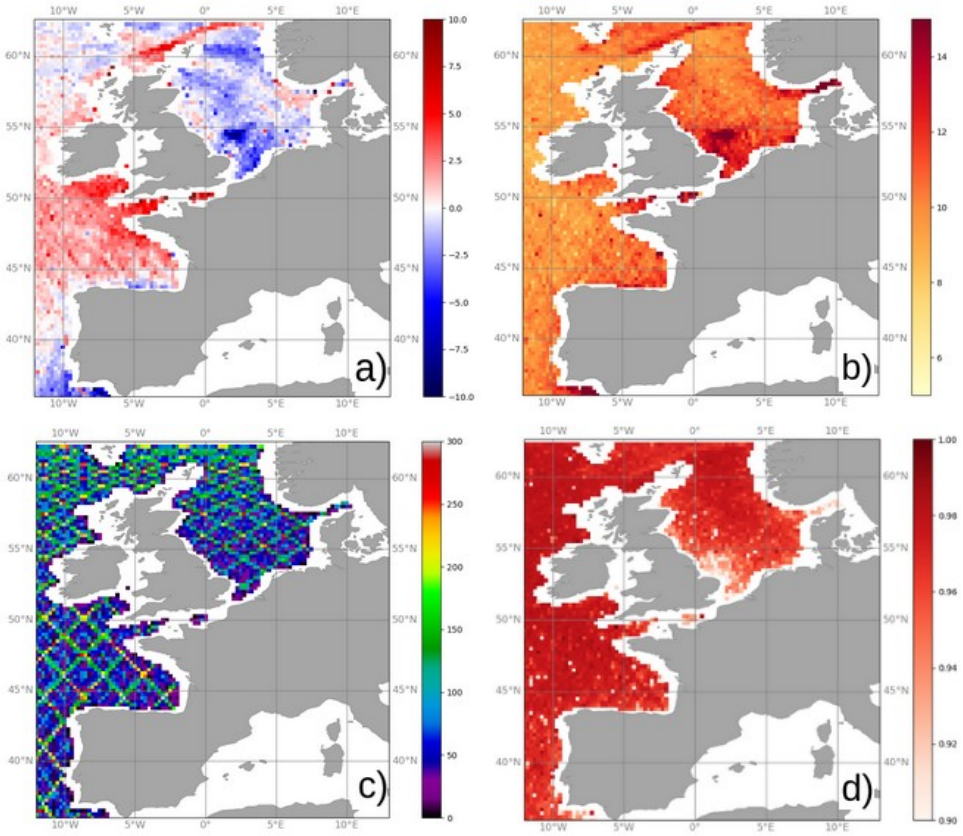

Figure 19 : yearly estimates averaged over 1993-2018

a) NB; b) NRMSE; c) matches-up; d) R

5.2 In-situ data

The *in-situ* validation dataset is composed of two types of data:

- Global integral parameters from InSituTAC database [5]
- Frequency spectra provided by national research centres at various locations along coasts (Cerema and Centrale Nantes in France, Marine Institute Ireland, EMEC in Scotland, Cefas Wavenet in the UK)

The validation on integral parameters is performed on selected locations across the EU: EMEC (BC), AMETS, SEM-REV, PIERRES NOIRES, and SmartBay. Integral parameters are significant wave height(H_{m0}), peak wave period (T_p), wave direction (θ_p,) and wave spreading (θ_s). The buoy data are archived using the Copernicus InsituTAC data standard. The standardized variable names are used to select validation parameters from the buoy records; the corresponding buoy

parameter names are VHM0, VTPK, VPED, VPSP. Not all buoys have all of these parameters, so the coverage varies by parameter.

The validation of the integrated parameters is applied on a month-by-month basis. Buoy data are cleaned using the relevant parameter QC flags (data samples not meeting the criteria are rejected). The remaining data are mapped onto the model's hourly timestamps using a nearest neighbor mapping with a minimum time difference threshold of ±1.5 hours. If fewer than 50% of the model timestamps are matched to buoy data then the buoy record is rejected, otherwise the validation parameters are calculated using the data flagged as "good" and the results tabulated.

Results on NB, NRMSE, SI and R are presented in the tables below. Data from the five sites were processed for the years 2015 to 2019 inclusive. The average values over all months at each site for each validation parameter are presented in the Table 9.

Table 9 : Parameters statistics per site (2015-2019)

(a) Significant Wave Height (H_{m0})

Site	B [m]	NB [%]	RMS [m]	NRMS [%]	SI [%]	R [%]
EMEC (BC)	0.02 (±0.03)	1.1 (±1.5)	0.27 (±0.07)	12.6 (±2.3)	11.1 (±2.3)	96.7 (±2.3)
AMETS	0.004 (± 0.07)	0.6 (±2.7)	0.35 (±0.10)	11.3 (±1.4)	10.2 (±1.1)	95.9 (±1.5)
SEM-REV	0.05 (±0.07)	3.5 (±4.3)	0.25 (±0.07)	13.9 (±2.6)	11.5 (±1.6)	96.2 (±2.0)
PIERRES NOIRES	0.24 (±0.06)	12.5 (±4.7)	0.37 (±0.09)	18.8 (±4.4)	12.3 (±1.6)	95.9 (±1.9)
SMART BAY	-0.20 (±0.05)	24.6 (±3.8)	0.25 (±0.06)	31.8 (±4.4)	17.3 (±2.7)	94.9 (±1.9)

(b) Peak Wave Period (T_p)

Site	B (s)	NB (%)	RMS (s)	NRMS (%)	SI (%)	R (%)
EMEC (BC)	-0.09 (±0.18)	-0.8 (±1.6)	1.5 (±0.2)	14.3 (±2.0)	13.9 (±2.0)	74.0 (±5.2)
AMETS	-0.20 (±0.19)	1.8 (±1.8)	1.28 (±0.24)	11.6 (±2.2)	11.2 (±2.2)	76.3 (±8.2)
SEM-REV	-0.03 (±0.22)	0.2 (±2.1)	1.70 (±0.42)	16.0 (±3.9)	15.5 (±3.7)	71.6 (±12.6)
PIERRES NOIRES	-0.13 (±0.24)	1.2 (±2.2)	1.60 (±0.60)	14.6 (±5.3)	14.1 (±4.7)	70.6 (±11.4)
SMART BAY	1.91 (±0.68)	27.1 (±8.5)	3.72 (±0.87)	52.8 (±9.7)	41.2 (±6.5)	40.9 (±10.5)

(c) Wave Direction (θ_p)

Site	B (°)	NB (%)	RMS (°)	NRMS (%)	SI (%)	R (%)
EMEC (BC)	-8,4 (±2.3)	-	-	-	-	69.0 (±13.2)
AMETS	-11.4 (±4.4)	-	-	-	-	75.1 (±12.7)
SEM-REV	-2.1 (±4.1)	-	-	-	-	60.3 (±16.0)
PIERRES NOIRES	1.4 (±6.2)	-	-	-	-	60.5 (±16.3)
SMART BAY	0.22 (±7.8)	-	-	-	-	52.2 (±22.3)

(d) Wave Spreading (θ_s)

Site	B (°)	NB (%)	RMS (°)	NRMS (%)	SI (%)	R (%)
EMEC (BC)	2.1 (±1.5)	7.4 (±5.1)	9.5 (±2.3)	33.3 (±7.1)	31.3 (±6.4)	39.1 (±9.9)
AMETS	-	-	-	-	-	-
SEM-REV	0.14 (±4.0 2)	0.6 (±14.3)	12.5 (±3.3)	44.7 (±100.6)	41.3 (±9.7)	24.2 (±17.8)
PIERRES NOIRES	7.5 (±3.4)	31.7 (±14.3)	12.3 (±3.5)	52.1 (±14.7)	39.3 (±8.8)	33.6 (±13.0)
SMART BAY	-	-	-	-	-	-

The sites chosen are all coastal; EMEC (BC) is on the west coast of the Orkneys, AMETS and SmartBay are on the west coast of Ireland, and SEM-REV and PIERRES NOIRES are on the west coast of Brittany. Among these five sites, two

were selected as they are relatively demanding for the model configuration. The SmartBay buoy is located in a sheltered area, close to the shore and PIERRES NOIRES is located in an area affected by strong tidal currents. For all sites the significant wave height is accurately predicted with the largest bias occurring at the PIERRES NOIRES and SmartBay sites. The peak wave period is also relatively well predicted (R<80) even though a larger RMS error is observed at the SmartBay site. Assessment of this parameter is however highly sensitive to the frequency discretization of the model and instruments as well as to the wind temporal and spatial resolution used to force the model. Mean period T02, showing less variability, will be investigated in the future. The peak direction shows a limited bias for the sites located in the Bay of Biscay and facing the open ocean as well as for the SmartBay site where the buoy is closer to the shore and sheltered. However, correlation for this latter is poorer. Agreement at AMETS is not as good (B>10°). The directional spreading was only available for the two sites in the Bay of Biscay. The RMS error is of about 12.5° and the correlation is poor. A larger bias is observed at PIERRES NOIRES where the influence of strong tidal currents occurring at that location is to be further investigated. It must be noted that the directional spreading as already been observed as the least well predicted parameter used to define the spectrum. These results are based on parameters integrated across the full wave spectrum, there are indications that integrated parameters based on spectral partitions will produce more consistent results for the wave period and directional data. Work is on-going to generate the statistics for parameters integrated by spectral partition.

The validation of frequency spectra is performed through the comparison of the modeled annual energy as a function of frequency against in-situ data provided by 26 buoys available over the domain: 8 buoys are located along the west coast of France, 3 are located in Irish waters and 15 around the UK, including 4 buoys at EMEC. Results are presented for 3 representative open sea test sites, AMETS, EMEC and SEM-REV. The spectral content can be considered as the sum of independent frequency bands, and the content in each band over time creates independent time series. Thus, the statistical estimators of error can be used at each bandwidth over wave energy spectrum.

Using the wave power per unit width J [W.m^{-1}] defined from the spectral density E and associated group velocity, the spectral quantity for a given frequency and bandwidth is defined as:

$$J(f_i, \Delta f_i) = \int_{f_i - \Delta f_i}^{f_i + \Delta f_i} \rho g C_g(f) E(f) df$$

The wave power per unit width is computed in frequency for buoy and model data. Comparisons between model output and measured quantities for three locations corresponding to ORE test sites are presented on Figure 20 for *J(f)* over the whole duration of the concomitant periods at each location. Error estimators are presented on Figure 21.

At low frequency, below 0.1 Hz, the discrepancies between modeling and measurement are more pronounced, especially at SEM-REV site which is in shallower water (34 m) compared to AMETS and EMEC (respectively 103 and 60 m depth). The maximum error in terms of NRMSE, NBIAS is reached for 0.04 Hz (i.e. wave periods of 25 s) for the deepest sites and 0.05-0.06 Hz (i.e. wave periods between 16 and 20 s) at SEM-REV.

This seems to indicate that the complex processes at stake at those intermediate to shallow depths such as refraction, dissipation by bottom friction, non-linear transfers or interaction with coastal flows remain difficult to accurately describe in the numerical model.

The high frequencies (above 0.1 Hz) are well resolved with NRMSE below 30% at deepest sites and below 40% at SEM-REV. The NBIAS is below 15% at SEM-REV and 5% for the deepest sites.

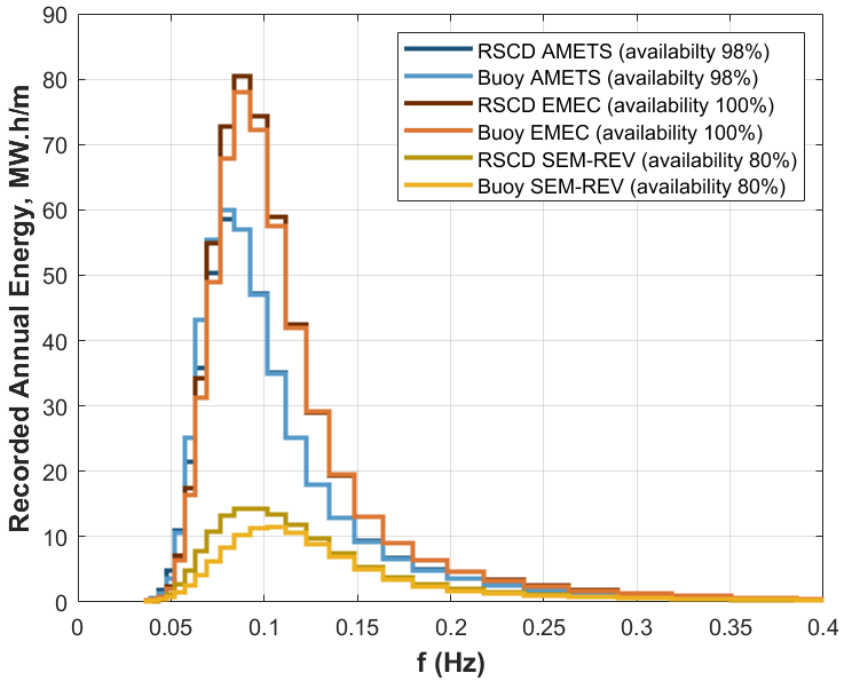

Figure 20 : Mean annual available wave energy in frequency from measurements and RESOURCECODE at three EU test sites locations in 2017

Finally, the spectral error on the annual energy shows that the model is underestimating the measurements at AMETS by 3.7%, overestimating by 4.2% at EMEC and 22.8% at SEM-REV.

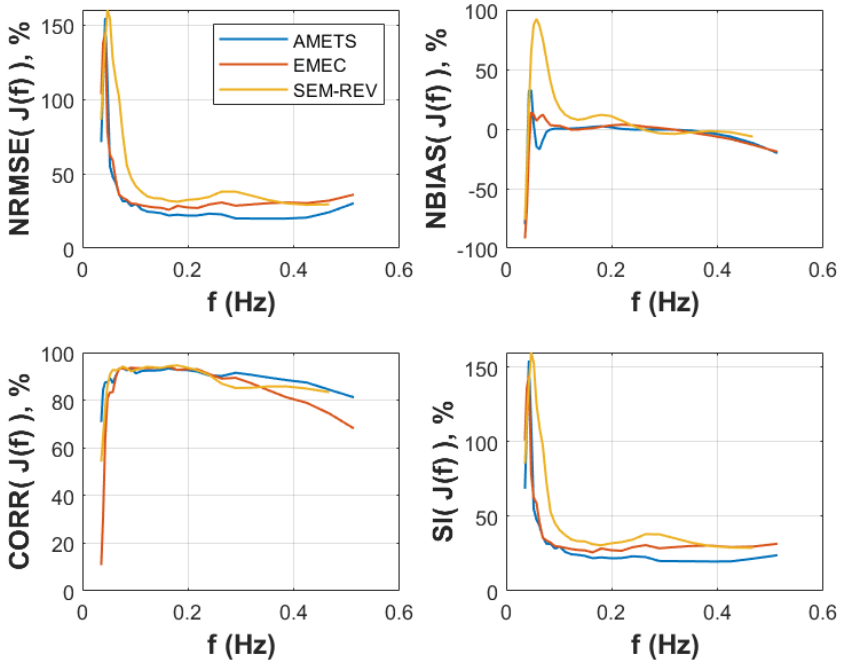

Figure 21 : NRMSE, NBIAS, CORR and SI of the spectral power resource between measurements and RESOURCECODE in 2017

6 Data usage, warnings and restrictions

6.1 Current and water level

Water velocities and levels have been produced based on tidal atlases which were generated from different hydrodynamics models and having different spatial resolution, the degree of confidence of this data is highly related to the location on the grid. As an example, around Orkney islands (see Figure 22), the complexity of the coastline and the coarse grid (2km resolution) used for tidal harmonics generation imply large inconsistencies in current and water levels used in the wave model.

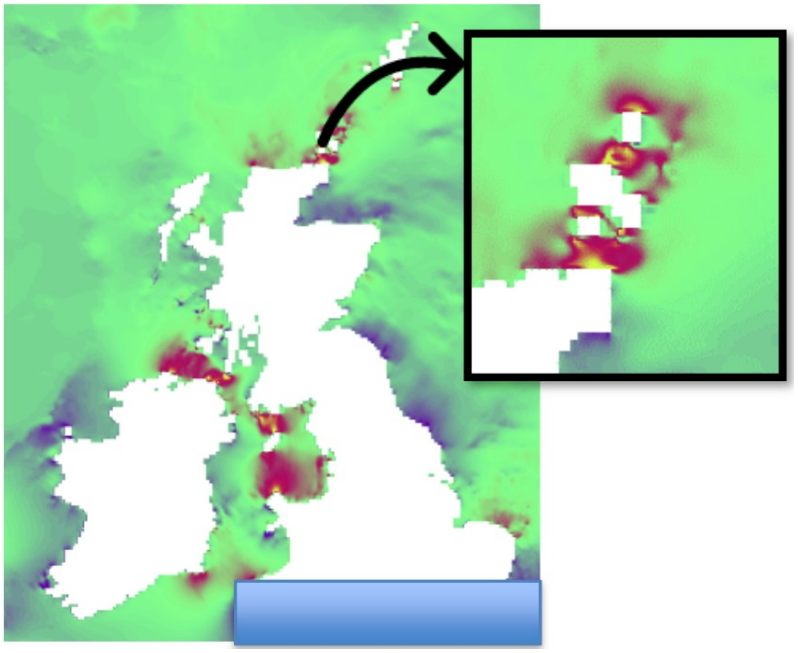

Figure 22 : Water velocities zoom on Orkneys

By comparing with a high-resolution hydrodynamic model “Scottish Shelf Waters Model”, it clearly highlights the low accuracy in complex areas.

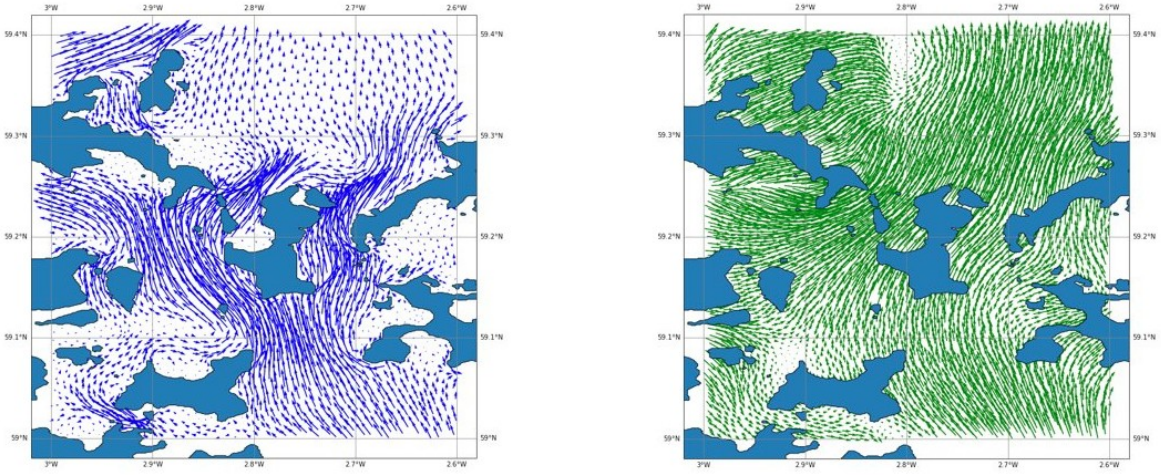

Figure 23 : Water velocities and directions

Left image: output from hydrodynamic model Scottish Shelf Waters. Right image: output from WW3 model.

6.2 Very shallow waters and harbor studies

The spectral model WAVEWATCH-III ®, which is a phase-averaged wave model, is design to solve the wave action equation from deep to shallow whereas studies in the surf zone, very shallow water and harbor area are out of the scope. A phase-resolved wave model is highly required for these studies. However, directional spectra from this database be can used as open boundaries.

6.3 Coastline contours and depth

Extra coarsening, up to 1200 [m], removal of islands, and sections' trimming were applied at the fjords along the Norwegian coast and the Frisian islands along Nederland and German coasts to simplify this area (which are out of the scope of the present project).

All coastlines' vertical coordinates were set to 2 [m] depth to avoid unrealistic wave height (Hs) gradients in extremely shallow water conditions, and to prevent excessive dry nodes effect in the mesh due to tidal levels variations. This consideration is especially important in areas with large tide coefficients where the integral wave parameters could be inaccurate at the nodes along the coastline contours.

7 How to cite

The RESOURCECODE wave dataset is registered under the DOI:

Accensi Mickael (2022). RESOURCECODE. IFREMER
https://doi.org/10.12770/d089a801-c853-49bd-9064-dde5808ff8d8

The model configuration and validation are described in the article:

Accensi Mickael, Alday Gonzalez Matias Felipe, Maisondieu Christophe, Raillard Nicolas, Darbynian David, Old Chris, Sellar Brian, Thilleul Olivia, Perignon Yves, Payne Gregory, O'Boyle Louise, Fernandez Leandro, Dias Frederic, Chumbinho Rogerio, Guitton Gilles (2021). ResourceCODE framework: A high-resolution wave parameter dataset for the European Shelf and analysis toolbox. Proceedings of the 14th European Wave and Tidal Energy Conference 5-9th Sept 2021, Plymouth, UK. ISSN: 2706-6940 (online) 2706-6932 (CD-ROM) 2706-6932 (Print). pp.2182-1-2182-9. https://archimer.ifremer.fr/doc/00736/84812/

Both references must be cited to provide references of the RESOURCECODE database in your papers and publications.

8 References

Alday Matias, Accensi Mickael, Ardhuin Fabrice, Dodet Guillaume (2021). A global wave parameter database for geophysical applications. Part 3: Improved forcing and spectral resolution. Ocean Modelling, 166, 101848 (19p.).

Ardhuin, F., and A. Roland, 2012. Coastal wave reflection, directional spread, and seismoacoustic noise sources, J. Geophys. Res., 117, C00J20.

Ardhuin, F., Tournadre, J., Queffelou, P., Girard-Ardhuin, F., 2011. Observation and parameterization of small icebergs: drifting breakwaters in the Southern Ocean. Ocean Modelling 39, 405–410.

Ardhuin Fabrice, Chapron Bertrand, Collard Fabrice (2009). Observation of swell dissipation across oceans. Geophysical Research Letters (GRL), 36(L06607), 1-5.

Ardhuin, F., Rogers, E., Babanin, A., Filipot, J.-F., Magne, R., Roland, A., van der Westhuysen, A., Queffeulou, P., Lefevre, J.-M., Aouf, L., Collard, F., 2010. Semi-empirical dissipation source functions for wind-wave models: part I, definition, calibration and validation. J. Phys. Oceanogr. 40 (9), 1917–1941.

Bidlot, J., Janssen, P., Abdalla, S., 2005. A revised formulation for ocean wave dissipation in CY25R1. Tech. Rep. Memorandum R60.9/JB/0516, Research Department, ECMWF, Reading, U. K.

Bidlot, J., Janssen, P., Abdalla, S., 2007. A revised formulation of ocean wave dissipation and its model impact. Tech. Rep. Memorandum 509, ECMWF, Reading, U. K.

Boudière, E., Maisondieu, C., Ardhuin, F., Accensi, M., Pineau-Guillou, L., Lepesqueur, J., 2013. “A suitable metocean hindcast database for the design of marine energy converters”. Int. J. Mar. Energy 28 (3–4), e40–e52.

Carrère, L., Lyard, F., Cancet, M., & Guillot, A. (2015, April). FES 2014, a new tidal model on the global ocean with enhanced accuracy in shallow seas and in the Arctic region. In EGU general assembly conference abstracts (p. 5481).

Copernicus Marine In Situ Tac Data Management Team, 2020. Product User Manual for multiparameter Copernicus In Situ TAC (PUM).

Dee, D. P., Uppala, S. M., Simmons, A. J., Berrisford, P., Poli, P., Kobayashi, S., Andrae, U., Balmaseda, M. A., Balsamo, G., Bauer, P., Bechtold, P., Beljaars, A. C. M., van de Berg, L., Bidlot, J., Bormann, N., Delsol, C., Dragani, R., Fuentes, M., Geer, A. J., Haimbergere, L., Healy, S. B., Hersbach, H., Holm, E. V., Isaksena, L., Køallberg, P., Kohler, M., Matricardi, M., McNally, A. P., Monge-Sanz, B. M., Morcrette, J.-J., Park, B.-K., Peubey, C., de Rosnay, P., Tavolato, C., Thepaut, J.-N., Vitart, F., 2011. The era-interim reanalysis: configuration and performance of the data assimilation system. Quart. Journ. Roy. Meteorol. Soc. 137, 553–597.

Dodet, G., Piolle, J.-F., Quilfen, Y., Abdalla, S., Accensi, M., Ardhuin, F., Ash, E., Bidlot, J.-R., Gommenginger, C., Marechal, G., Passaro, M., Quartly, G., Stopa, J., Timmermans, B., Young, I., Cipollini, P., Donlon, C., 2020. The sea state cci dataset v1: towards a sea state climate data record based on satellite observations. Earth System Sciences. Data 12, 1929–1951.

Foreman, M. G. G., Cherniawsky, J. Y., & Ballantyne, V. A. (2009). Versatile Harmonic Tidal Analysis: Improvements and Applications, Journal of Atmospheric and Oceanic Technology, 26(4), 806-817. Retrieved Sep 9, 2021, from https://journals.ametsoc.org/view/journals/atot/26/4/2008jtecho615_1.xml

Gallagher, S., Tiron, R. & Dias, F. (2014) A long-term nearshore wave hindcast for Ireland: Atlantic and Irish Sea coasts (1979–2012). Ocean Dynamics 64, 1163–1180.

Girard-Ardhuin, F., Ezraty, R., 2012. Enhanced arctic sea ice drift estimation merging radiometer and scatterometer data. IEEE Trans. on Geosci. and Remote Sensing 50, 2639–2648.

Grant, W. D., and O. S. Madsen (1979), Combined wave and current interaction with a rough bottom, J. Geophys. Res., 84(C4), 1797-1808.

Hasselmann, S., Hasselmann, K., Allender, J., Barnett, T., 1985. Computation and parameterizations of the nonlinear energy transfer in a gravity-wave spectrum. Part II: Parameterizations of the nonlinear energy transfer for application in wave models. J. Phys. Oceanogr. 15, 1378–1391.

Hersbach, H., Bell, B., Berrisford, P., Hirahara, S., Horányi, A., Muñoz-Sabater, J., Nicolas, J., Peubey, C., Radu, R., Schepers, D., Simmons, A., Soci, C., Abdalla, S., Abellan, X., Balsamo, G., Bechtold, P., Biavati, G., Bidlot, J., Bonavita, M., Chiara, G. D., Dahlgren, P., Dee, D., Diamantakis, M., Dragani, R., Flemming, J., Forbes, R., Fuentes, M., Geer, A., Haimberger, L., Healy, S., Hogan, R. J., Hólm, E., Janisková, M., Keeley, S., Laloyaux, P., Lopez, P., Lupu, C., Radnoti, G., de Rosnay, P., Rozum, I., Vamborg, F., Villaume, S., Thépaut, J., 2020. “The ERA5 global reanalysis”. Quart. Journ. Roy. Meteorol. Soc. 146, 1999–2049.

Janssen, P. A. E. M., 1991. Quasi-linear theory of wind wave generation applied to wave forecasting. J. Phys. Oceanography. 21, 1631-1642, see complements by D. Chalikov, J. Phys. Oceanography. 1993, vol. 23 pp. 1597-1600.

Lazure P., Dumas F., 2008. An external-internal mode coupling for a 3D hydrodynamical model for applications at regional scale (MARS). Advances In Water Resources, 31(2), 233-250.

Leckler, F., 2013. Observation et modélisation du déferlement des vagues. Ph.D. thesis, Université Européenne de Bretagne, École doctorale des Sciences de la Mer, Brest, France.

Leonard, B. P., 1991. The ULTIMATE conservative difference scheme applied to unsteady one-dimensional advection. Computational Methods Applied in Mechanical Engineering 88, 17-74.

Perignon, Y. (2017). Assessing accuracy in the estimation of spectral content in wave energy resource on the French Atlantic test site SEMREV. Renewable Energy, 114, 145-153.

Perignon, Y., & Maisondieu, C. (2017, August). Assessing accuracy of hindcast spectral content in the estimation of wave energy resource. In European Wave and Tidal Energy Conference.

Pineau-Guillou, L., 2013. Validation des atlas de composantes harmoniques de hauteurs et courants de marée. (https://marc.ifremer.fr/content/download/7861/41823/file/2013_06_12_rap_valid_atlas_V1.pdf)

Pineau-Guillou Lucia, Ardhuin Fabrice, Bouin Marie-Noëlle, Redelsperger Jean-Luc, Chapron Bertrand, Bidlot Jean-Raymond, Quilfen Yves (2018). Strong winds in a coupled wave-atmosphere model during a North Atlantic storm event: evaluation against observations. Quarterly Journal Of The Royal Meteorological Society, 144(711 Part.B), 317-332.

Roland, A., Development of WWM II: Spectral Wave Modelling on Unstructured Meshes, Ph. D. thesis, Inst. of Hydraul. and Wave Resour. Eng., Darmstadt University of Technology, Germany, 2008.

Roland, A. Cucco, A., Ferrarin, C., Hsu, T.-W., Liau, J.-M., Ou, S.-H., Umgiesser, G., Zanke, U., On the development and verification of 2-D coupled wave-current model on unstructured meshes, J. Mar. Syst. 78 (2009) S244–S254.

Roland Aron, Ardhuin Fabrice (2014). On the developments of spectral wave models: numerics and parameterizations for the coastal ocean. Ocean Dynamics, 64(6), 833-846.

The European Marine Energy Centre (2020). BC-DWR-E-2017, EMEC Datawell Waverider data at full scale wave test site at Billia Croo, Orkney, UK. SEANOE.

Stopa, J. E., Ardhuin, F., Stutzmann, E., Lecocq, T., 2019. Sea state trends and variability: consistency between models, altimeters, buoys, and seismic data (1979-2016). J. Geophys. Res. 124, in press.

The WAVEWATCH III ® Development Group, 2019. User manual and system documentation of WAVEWATCH III ® version 6.07. Tech. Note 333, NOAA/NWS/NCEP/MMAB, College Park, MD, USA, 465 pp. + Appendices.

Tournadre, J., Bouhier, N., Girard-Ardhuin, F., Remy, F., 2016. Antarctic iceberg distributions 2002–2010. J. Geophys. Res. 121, 327–349.

Cerema. Fiches synthétiques de mesure des états de mer - Tome 1 – Mer du Nord, Manche et Atlantique - Janvier 2021Cerema, 2021. Collection : Données. ISBN : 978-2-37180-497

“This collaborative project has received support under the framework of the OCEANERA-NET COFUND project, with funding provided by national/ regional sources and co-funding by the European Union´s Horizon 2020 research and innovation programme.”

www.resourcecode.info